Ab initio study of energetics and magnetism of Fe, Co, and Ni along the trigonal deformation path

M. Zelený,[1,2] M. Friák,[1,3,4,5] and M. Šob[1,5,6]

[1]*Institute of Physics of Materials, Academy of Sciences of the Czech Republic, Žižkova 22, CZ-616 62 Brno, Czech Republic*
[2]*COMP/Department of Applied Physics, Aalto University School of Science, P.O. Box 11100, FI-00076 Aalto, Finland*
[3]*Max-Planck-Institut für Eisenforschung GmbH, Max-Planck-Strasse 1, D-40237 Düsseldorf, Germany*
[4]*Institute of Condensed Matter Physics, Faculty of Science, Masaryk University, Kotlářská 2, CZ-611 37 Brno, Czech Republic*
[5]*Central European Institute of Technology, CEITEC MU, Masaryk University, Kamenice 5, CZ-625 00 Brno, Czech Republic*
[6]*Department of Chemistry, Faculty of Science, Masaryk University, Kotlářská 2, CZ-611 37 Brno, Czech Republic*

(Received 7 February 2011; revised manuscript received 21 March 2011; published 24 May 2011)

A detailed theoretical study of structural and magnetic behavior of iron, cobalt, and nickel along the trigonal transformation paths at various volumes per atom is presented. The total energies are calculated by a spin-polarized full-potential linearized augmented plane wave method within the generalized gradient approximation and are displayed in contour plots as functions of trigonal c/a ratio and volume per atom. The borderlines between various magnetic modification are shown for Fe and Ni. In the case of Ni, these phase boundaries between nonmagnetic and ferromagnetic phases occur even at the experimental value of volume per atom. On the other hand, Co keeps its ferromagnetic order in the whole region of the volume and shape deformation studied. Fe does not exhibit any transition between the ferromagnetic and nonmagnetic arrangement, but at low volumes per atom around the fcc structure, phase boundaries between the ferromagnetic high-spin, ferromagnetic low-spin, and antiferromagnetic states have been found. Fe and Co exhibit minima on the curve of the energy difference between ferromagnetic (FM) and nonmagnetic states in the same areas where Ni loses its FM ordering. Both structures do not exhibit any higher symmetry, but there is a coalescence of the second and third and fifth and sixth coordination spheres ($c/a = 1.27$) or of the third and fourth coordination spheres ($c/a = 2.83$).

DOI: 10.1103/PhysRevB.83.184424 PACS number(s): 63.70.+h, 71.15.Nc, 75.50.−y

I. INTRODUCTION

Iron, cobalt, and nickel have been for a long time at the center of attention because of their unique magnetic properties. In particular, ferromagnetism in these metals is very important not only for their magnetic properties *per se*, but because it stabilizes the body-centered cubic (bcc) ground-state structure of Fe and the hexagonal closed-packed (hcp) ground-state structure of Co. Had the magnetism been absent, the nonmagnetic state of both elements would exhibit the same structure as the corresponding 4*d* and 5*d* metals in the same columns of the Periodic Table, i.e., Fe would have the hcp structure in analogy with Ru and Os and Co would crystallize in the face-centered cubic (fcc) structure in analogy with Rh and Ir. The origin of ferromagnetism in Fe, Co, and Ni consists in the high density of states at the Fermi level of nonmagnetic configurations in these metals, which leads to the spin polarization of the valence band.[1–4]

Recently, a great deal of attention was also paid to thin films of these metals, because they have a wide use in practical applications, especially in data storage devices. In fact, thin films show how to stabilize 3*d* metals in deformed structures, which can exhibit partially or completely different magnetic behavior than their ground states. A nice illustrative example showing the changes in magnetic behavior is elemental iron. If it is deposited on the Cu(001) substrate, its fcc structure with antiferromagnetic (AFM) ordering is stabilized[5,6] similarly as in iron precipitates embedded into a Cu matrix.[7,8] This stabilization happens primarily due to a high deformation of the film or of the precipitate, which keeps it coherent with the substrate or with the matrix. It turns out that the substrate or the matrix just mechanically constrain the material of the film or of the precipitate in those deformed structures. For thin iron films, this was reliably demonstrated with the help of *ab initio* calculations,[9] which provide a very good tool for the study of these highly deformed states. Another example of stabilized nonequilibrium configurations is Ni and Co overlayers with the bcc structure, which were prepared on a GaAs (001) substrate.[10,11] In addition, a Co film with a tetragonally distorted bcc structure was reported on Pd and Pt substrates.[12,13]

Many theoretical studies are focused on the behavior of 3*d* and other metals along the tetragonal deformation path (also called the Bain's path), which is accomplished by an uniaxial deformation along the [001] direction. This path connects the bcc and fcc structures[9,14,15] and is suitable for a description of the geometry of the structures that occur in thin films on the (001) substrates (mainly with the fcc structure). However, there is no significant change of magnetic properties of Ni and Co along this path, as shown in previous studies.[16,17] Consequently, most Ni and Co thin films on fcc (001) substrates studied up to now prefer ferromagnetic ordering (Ref. 18 and references therein). Only Fe changes magnetic ordering from ferromagnetic to antiferromagnetic along this path[9] or to a spin-spiral structure, when noncollinear arrangement is admitted.[19]

An interesting alternative is provided by films on (111) fcc substrates, where they exhibit a trigonally distorted fcc structure or hcp structure.[20] Here, for example, Ni with hcp structure subjected to a large biaxial deformation loses its ferromagnetism, but these deformed states are already beyond the stability limit of Ni films on fcc (111) substrates due to very large lattice mismatch.[21] Highly trigonally deformed states can be unstable for the same reason and are experimentally hardly accessible. Nevertheless, the study of these states can bring

a lot of information about magnetic properties of 3*d* metals under large deformations.

Similarly as tetragonally deformed structures may be found along the Bain's deformation path, the trigonally deformed structures occur along the trigonal deformation path, which continually connects the bcc and fcc structures as well but via trigonal deformation. This deformation path includes also the simple cubic (sc) structure in between (see, e.g., Refs. 15 and 22–26). A few *ab initio* studies of 3*d* metals have already been performed for structures along this path,[27,28] including an investigation of magnetic anisotropy energy in Fe, Co, and Ni,[29] but a detailed comparative study of energetics and magnetism of these 3*d* metals along trigonal deformation paths is still missing.

The purpose of this paper is to fill in this gap. We present a detailed and comprehensive analysis of the total energy and magnetic behavior of ferromagnetic 3*d* metals along trigonal deformation paths at various volumes, identify the stable and metastable phases of these metals, and find the phase boundaries between ferromagnetic and nonmagnetic modifications. On the basis of analysis of the density of states, we also provide an explanation of the differences between the behavior of these metals along trigonal deformation paths.

II. COMPUTATIONAL DETAILS

As we have mentioned in the Introduction, bcc, sc, and fcc structures are related by means of trigonal deformation and may be continually connected by a trigonal deformation path. We may start with the bcc structure and consider it as a trigonal one with the c/a ratio equal to 1. Here c is the length of a line segment in the lattice measured along the [111] direction and a is the length of a line segment measured along any perpendicular direction. If $c/a \neq 1$, the structure becomes trigonal except for $c/a = 2$, when we attain the simple cubic (sc) structure, and $c/a = 4$, which corresponds to the fcc structure. Structures along a trigonal transformation path may be described also as hexagonal structures with three atoms in the basis.[21]

The structures at $c/a = 1$, 2, and 4 represent the only higher-symmetry structures encountered along the trigonal deformation path. It turns out that the derivative of the total energy with respect to the parameter describing the path is zero at these points and the total energy exhibits so-called symmetry-dictated stationary points, mostly minima or maxima.[30] Of course, other stationary points may occur that are not dictated by symmetry; they reflect properties of a specific material under study.

In the present paper, we calculate the total energy of nonmagnetic (NM), ferromagnetic (FM), and antiferromagnetic (AFM) iron, cobalt, and nickel along the trigonal deformation paths keeping the volume per atom constant. In the AFM structures, we suppose an opposite orientation of magnetic moments at the consecutive (111) planes, which corresponds, for example, to the AFMII ordering of Ref. 31. The region of volumes per atom studied extends from $V/V_{\mathrm{exp}} = 0.85$ to $V/V_{\mathrm{exp}} = 1.25$ (V_{exp} is the experimental volume per atom).

For the total-energy calculations, we utilize the full-potential linearized augmented plane waves method implemented in the WIEN2K code.[32] The calculations are performed using the generalized gradient approximation (GGA)[33] in a scalar-relativistic mode, i.e., without inclusion of the spin-orbit coupling. Our test calculations revealed that the spin-orbit coupling does not affect the behavior and the values of total energies and magnetic moments in any significant way. The number of **k** points in the irreducible Brillouin zone is equal to 2500, including structures with higher symmetry, which were treated on equal footing to the other structures (i.e., with the help of the hexagonal unit cell). The muffin-tin radius of atoms of 2.0 a.u. is kept constant for all calculations, the product of the muffin-tin radius and the maximum reciprocal space vector, $R_{\mathrm{MT}}k_{\mathrm{max}}$ (related to the cutoff of the plane wave basis), is equal to 9, and the maximum value of l for the waves inside the atomic spheres, l_{max}, is set to 12 for iron, to 11 for cobalt, and to 9 for nickel. The largest reciprocal vector **G** in the charge Fourier expansion, G_{max}, is set to 16. For a correct treatment of 3*p* semicore states, the augmented plane wave plus local-orbital extension[34] is used. The energy convergence criterion is 1×10^{-6} Ry/atom and, on the basis of the convergence tests with respect to the number of **k** points, the error in calculated total energies may be estimated to be less than 5×10^{-5} Ry/atom.

III. RESULTS

Figure 1 displays the variation of the total energy of iron (a), cobalt (b), and nickel (c) at the experimental lattice volumes of these metals in FM states. Our calculated equilibrium lattice parameter of bcc ferromagnetic Fe, $a_{\mathrm{eq}} = 5.35$ a.u., is a bit lower as compared to the experimental value $a_{\mathrm{exp}} = 5.42$ a.u.[35] However, this is in accordance with other recent theoretical results (see, e.g., Ref. 36) as well as with the fact that the exchange-correlation functional (GGA) used here[33] is well known to slightly underestimate the equilibrium volume of bcc FM Fe. Agreement for fcc Co ($a_{\mathrm{eq}} = 6.65$ a.u. and $a_{\mathrm{exp}} = 6.68$ a.u.[37]) and Ni ($a_{\mathrm{eq}} = 6.66$ a.u. and $a_{\mathrm{exp}} = 6.65$ a.u.[35]) is much better. Corresponding magnetic moments are shown in Fig. 2.

The NM and FM states exhibit symmetry-dictated extrema of total energy at $c/a = 1$, 2, and 4: minima correspond to bcc and fcc structures and the maximum to the sc structure. However, the curve for FM Fe states is very flat around the fcc structure and may contain a very flat local maximum at $c/a = 4$ accompanied by a very shallow local minima at each side, similarly as in Nb, Mo, and W, where these features are much more pronounced.[15,38–40] In Fe and Co, the FM ordering has the lowest energy in the whole interval of c/a studied. However, in Ni, we may observe two intervals of c/a ($1.20 < c/a < 1.45$ and $2.70 < c/a < 3.10$), where the ferromagnetic ordering is lost and no FM states occur—the corresponding magnetic moment is zero within the error limits. It is interesting that in the same intervals the magnetic moment of FM Co reaches the highest values along the whole curve, whereas for FM Fe and FM Ni the highest magnetic moments are found in the neighborhood of the fcc structure.

Energy profiles for AFM states are very similar to those for the NM and FM states with one important exception. The minima that are close to the fcc structure do not lie exactly at $c/a = 4$, but are slightly shifted (to $c/a = 4.10$, 4.05, and 4.01 for Fe, Co, and Ni, respectively), because they are not dictated

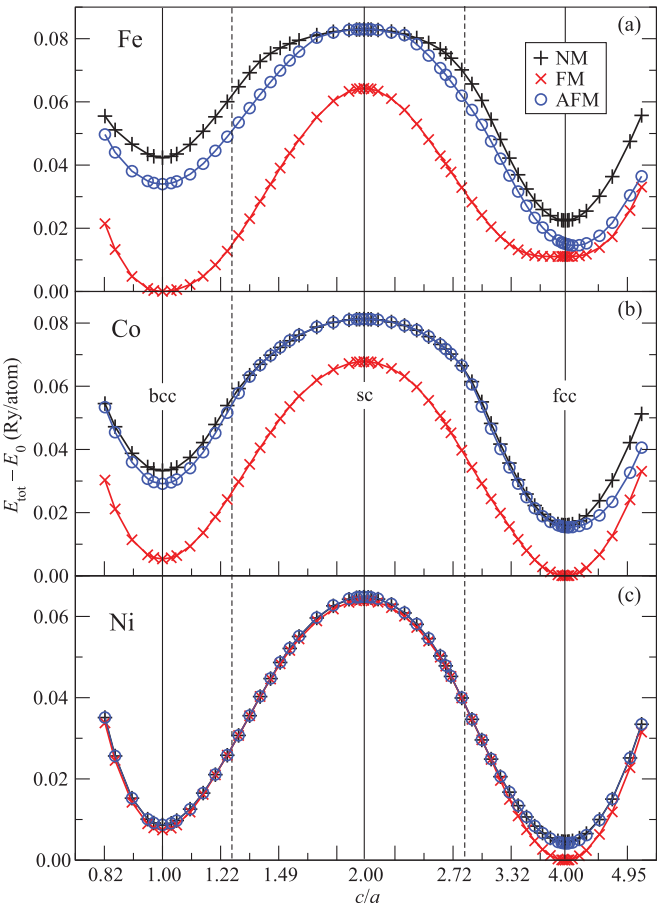

FIG. 1. (Color online) Total energy of Fe, Co, and Ni as a function of c/a along the trigonal deformation path at the experimental volume per atom. The energies are given with respect to the energies of the equilibrium ground states; the horizontal axis has a logarithmic scale. The vertical dashed lines correspond to $c/a = 1.27$ and $c/a = 2.83$, where some coordination spheres in the trigonal structure join together (see Fig. 5).

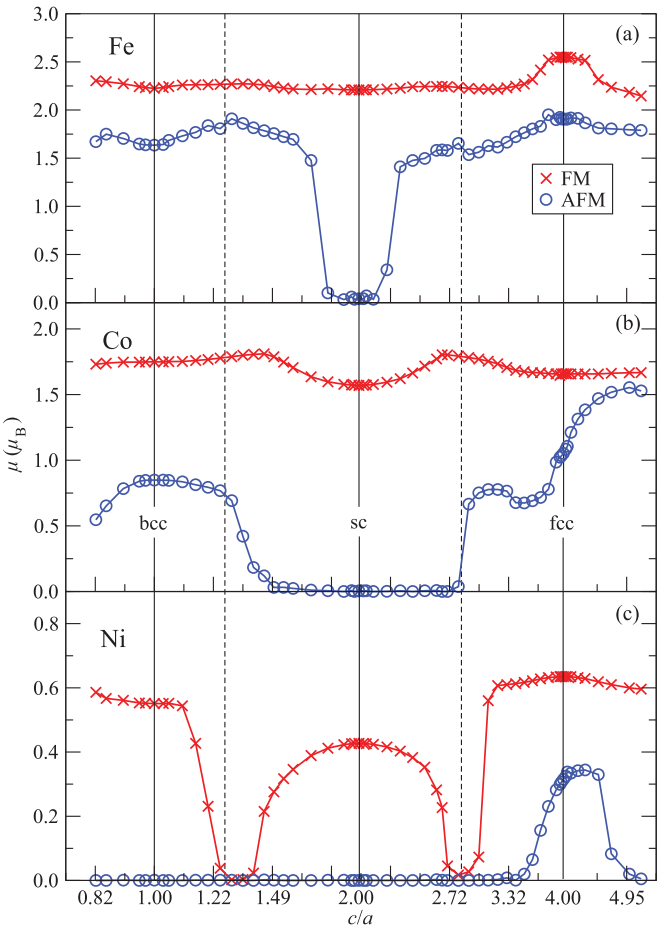

FIG. 2. (Color online) Magnetic moments of Fe, Co, and Ni as functions of c/a along the trigonal deformation path at the experimental volume per atom; the horizontal axis has a logarithmic scale. The vertical dashed lines correspond to $c/a = 1.27$ and $c/a = 2.83$ (see Fig. 5).

by symmetry. Namely, at $c/a = 4$, the atoms occupy the fcc lattice positions, but as the atoms with spins up and down are not equivalent, the resulting symmetry is still trigonal and no higher-symmetry structure occurs here. Further, the AFM states of Fe and Co degenerate to the NM states in the intervals $1.78 < c/a < 2.30$ and $1.45 < c/a < 2.80$, respectively, i.e., again, within error limits, the energy of the AFM states is the same as that of the NM states and the magnetic moment of the AFM states is zero. The interval of degeneration is slightly broader for Co than for Fe. For Ni, however, the AFM states have the same energy as the NM states along the whole curve except for the interval $3.80 < c/a < 4.50$.

Let us note that the experimentally found most stable magnetic configuration for fcc Fe is the paramagnetic state (so-called γ-Fe) that exists only at elevated temperatures. In order to stabilize the fcc Fe at ambient or low temperatures, epitaxial strains are typically applied to Fe by various substrates. Then the most stable magnetic state sensitively depends on, e.g., the temperature, the lattice parameter mismatch between the substrate and the film, preparation conditions, or even the thickness of the iron film (see, e.g., Refs. 18, 41–43, and references therein). The most stable state predicted by *ab initio* calculation is a spin-spiral configuration with the wave vector $q = (0,0,0.56)$. This configuration is very close to a collinear antiferromagnetic double-layer arrangement.[9,19] However, in that stable configuration, there is an opposite orientation of magnetic moments at the consecutive (001) planes, whereas we treat an AFM configuration with an opposite orientation of magnetic moments at the consecutive (111) planes here. That is why our total-energy profiles exhibit the FM configuration at $c/a = 4$ as the lowest-energy one.

To see the effect of volume changes, we have calculated total energies along the trigonal paths in a large interval of volumes and plotted these results in contour plots. Figure 3 displays the total energy of Fe, Co, and Ni as a function of c/a and volume per atom relative to the energy of the FM bcc (Fe), FM hcp (Co), and FM fcc (Ni) equilibrium states. Thick lines show the boundaries between different magnetic phases. In iron [Fig. 3(a)], the phase boundaries appear in the neighborhood of the fcc structure for volumes per atom $V/V_{exp} < 0.95$. If c/a is higher than 4.05, the AFM state has a lower energy in this region. For $c/a < 4.05$, iron still keeps the FM arrangement but magnetic moments strongly decrease from 2.2 μ_B to 1.5 μ_B, which corresponds to the transition from the high-spin (FM-HS) to the low-spin (FM-LS) ferromagnetic

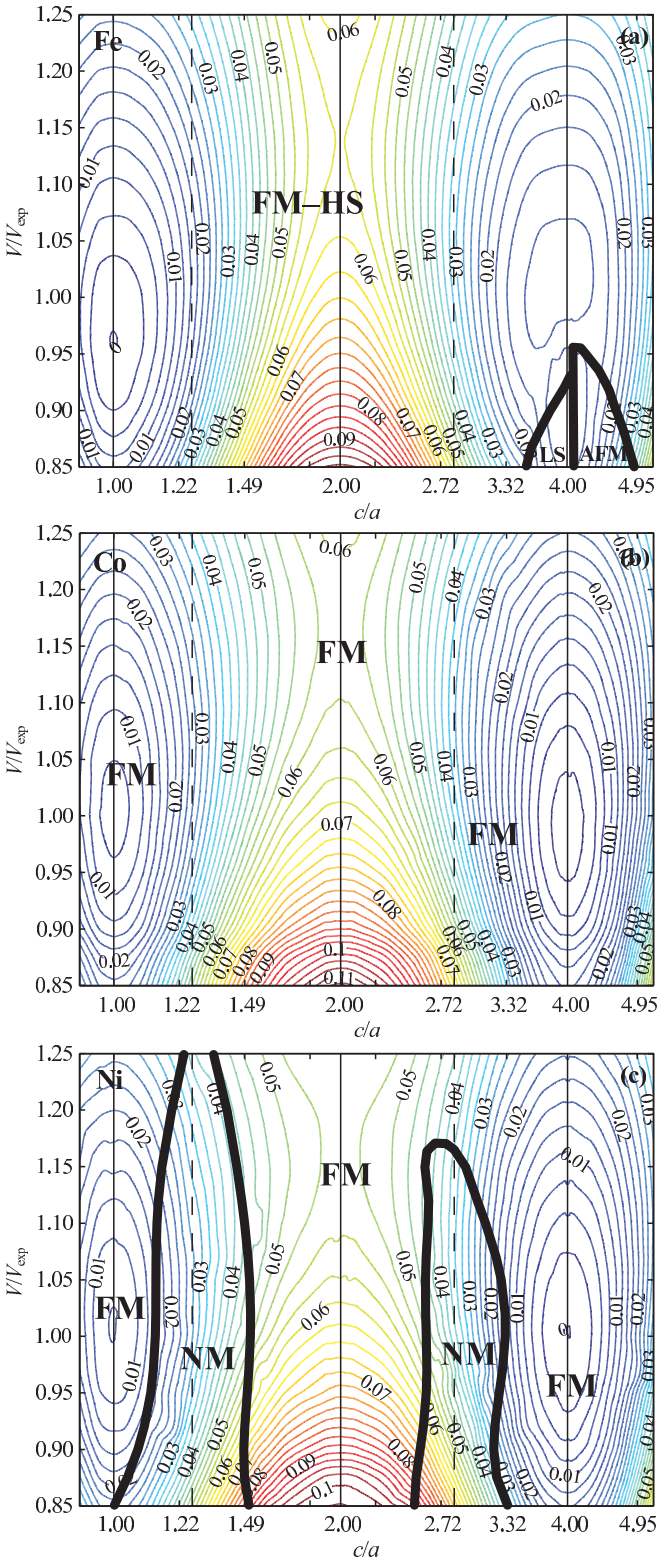

FIG. 3. (Color online) Total energy of iron, cobalt, and nickel as a function of c/a and volume along the trigonal deformation path relative to the equilibrium ground-state energy; the horizontal axis has a logarithmic scale. Only states with the minimum energy are shown. The contour interval is 0.0025 Ry/atom. Thick lines show boundaries between different magnetic phases; thin dashed vertical lines correspond to $c/a = 1.27$ and $c/a = 2.83$ (see Fig. 5).

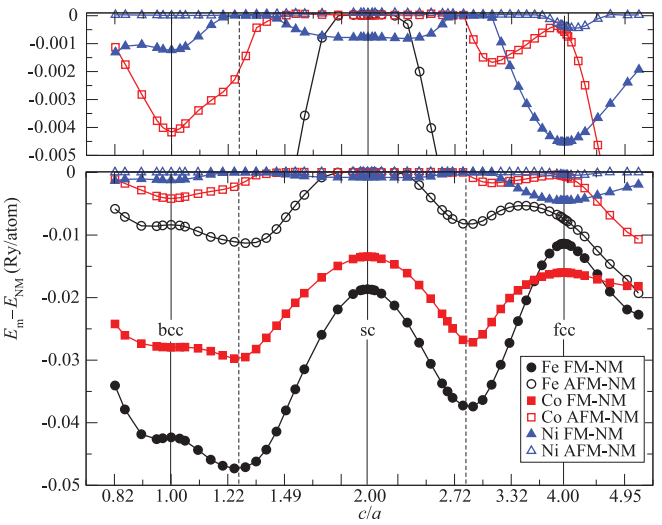

FIG. 4. (Color online) Energy differences between FM and NM states (full symbols) and between AFM and NM states (open symbols) as a function of c/a along the trigonal deformation path at the experimental volume per atom; E_m stands for E_{FM} or E_{AFM}. The horizontal axis has a logarithmic scale. The upper part of the figure shows details for small energies. Thin dashed vertical lines correspond to $c/a = 1.27$ and $c/a = 2.83$ (see Fig. 5).

state. This transition at lower volumes is characteristic of fcc FM Fe and was described in several previous works.[44–46] However, except for the region around the fcc structure for $V/V_{exp} < 0.95$, no other phase boundaries have been detected. Cobalt does not exhibit any magnetic transition under trigonal deformation in the whole region of volumes per atom and trigonal deformations studied.

On the other hand, nickel exhibits two nonmagnetic areas, which were found also at the experimental volume per atom. The first one is centered around $c/a \approx 1.25$ and extends from low volumes per atom up to $V/V_{exp} \approx 1.28$; the second one is found around $c/a \approx 2.9$ for $V/V_{exp} < 1.17$.

Comparison of energy differences between magnetic and nonmagnetic states can tell us much more about the properties of the systems studied. This comparison is shown in Fig. 4 at experimental volumes per atom. Energy differences between FM and NM states for Fe and Co exhibit a similar shape with two maxima corresponding to fcc and sc structures. At the third structure with a higher symmetry, namely bcc, Fe exhibits a flat maximum and Co a shallow minimum. More pronounced minima on these curves are located at the same positions, at $c/a = 1.27$ and at or close to $c/a = 2.83$, but these points do not correspond to any structure with a higher symmetry.

On the other hand, Ni behaves very differently. First, the FM-NM energy difference is much smaller. For fcc and bcc structure, it exhibits minima and not maxima. At the points where FM-NM energy differences for Fe and Co exhibit deep minima, we find zero values for Ni because these points occur in the middle of NM areas. For Co and Ni, the values of FM-NM energy differences strongly correlate with the values of magnetic moment. In the case of Fe, correlation is worse, because the global maximum of the FM-NM curve at the fcc structure corresponds to an area where magnetic moments have the highest values. This effect is related to a flat profile

of the total energies of FM states in this region [Fig. 1(a)] and may be connected to the presence of the HS-LS transition in a close neighborhood [Fig. 3(a)]. Energy differences between AFM and NM states for Fe have a very similar behavior as energy differences between FM and NM states. One exception is observed around $c/a = 4$, where the maximum is shifted from this point due to missing structure with a higher symmetry here. In addition, the AFM-NM energy differences exhibit zero values in the interval between $c/a = 1.82$ and $c/a = 2.34$, which corresponds to the degeneracy of AFM and NM states in this area. The same effect can be observed for Co, but here the area of degeneracy of AFM and NM states is much wider—practically between the same points where FM-NM energy differences exhibit their minima ($c/a = 1.27$ and $c/a = 2.83$). The AFM-NM energy differences for Ni are zero nearly along the whole deformation path, but around the fcc structure the negative values are slightly higher, which correlates with nonzero magnetic moments. A similar correlation between the magnetic moments of AFM states and AFM-NM energy differences can be observed for the other two metals as well.

IV. DISCUSSION

We have found two interesting structures on the trigonal deformation paths, which have indisputable influence on magnetic properties of deformed material and on the shape of total energy differences between various magnetic modifications. They are located at $c/a = 1.27$ and $c/a = 2.83$. Let us note that the manifestation of the presence of these structures is the strongest in Ni and the weakest in Fe, because Ni loses its magnetic ordering at these points, whereas in Fe changes in magnetic moments are hardly distinguishable (Fig. 2). In Fe and Co, pronounced minima on the curves of energy differences between FM and NM state may be observed (Fig. 4).

Let us recall that the symmetry of structures at $c/a = 1.27$ and $c/a = 2.83$ is only trigonal and no higher symmetry occurs here. However, if we look at the diagram of interatomic distances and coordination spheres (Fig. 5), we can see that there

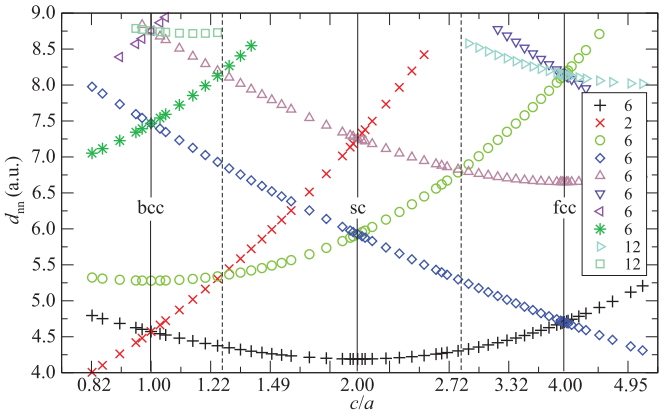

FIG. 5. (Color online) Interatomic distances in Ni as a function of c/a along the trigonal deformation path at the experimental volume per atom; the horizontal axis has a logarithmic scale. The numbers in the legend correspond to the number of atoms in coordination spheres. Thin dashed vertical lines correspond to $c/a = 1.27$ and $c/a = 2.83$, where some coordination spheres in the trigonal structure join together.

is a coalescence of some coordination spheres at those points (denoted by dashed vertical lines in Figs. 1–5). A coalescence of the second and third as well as the fifth and sixth coordination spheres occurs at $c/a = 1.27$, whereas the third and fourth spheres join at $c/a = 2.83$. Consequently, these two structures have an increased number of neighbors in their coordination spheres, but their symmetry remains trigonal and their space group is the same as that of the neighboring structures. Had these configurations had a higher symmetry, then this would be reflected by symmetry-dictated stationary points on the total energy profiles. However, the total energy dependencies do not exhibit any stationary behavior; only the values of $c/a = 1.27$ and 2.83 are close to the inflection points (Fig. 1). On the other hand, we can see distinct extrema in the FM-NM total energy differences at or close to these points (Fig. 4).

All three ferromagnetic metals studied here exhibit very different behavior at these two structures. Ni is nonmagnetic, whereas Co and Fe possess the lowest energy for the ferromagnetic state and Co has also the highest magnetic moment along the whole path close to these points. Fe in the AFM state exhibits a nonzero magnetic moment and a higher energy than the FM state. The energy of AFM Ni is the same as the energy of Ni in the NM state, which is the only state stable here. For Co these points are boundary points where magnetic moments of AFM states and the energy differences between AFM and NM states start reaching zero (Fig. 4).

These different behaviors can be understood on the basis of analysis of density of states (DOS). DOS for NM states of all metals are shown in Fig. 6. The shape of the DOS depends mainly on crystal structure, but its position with respect to the Fermi energy is determined by the number of electrons. Very high DOS of an NM state at the Fermi level indicates a tendency to stabilization of the FM state, which follows from the Stoner analysis.[47] NM Ni in the fcc structure ($c/a = 4$) exhibits a high density of states at the Fermi level ($N \approx 61$ states/Ry/atom) and this is the reason for FM ordering, because a high DOS at the Fermi level can be lowered by splitting into the up and down channels. NM Co and Fe possess also relatively high values of the DOS at the Fermi level ($N \approx 30$ states/Ry/atom). This is a smaller value than in the case of Ni, but still high enough, and both metals prefer the FM state over the NM one. If the fcc structure is compressed along the [111] direction (let us keep the volume per atom constant at its experimental value), the high cubic symmetry is lost as well as the degeneracy of the e_g and t_{2g} d orbitals. At $c/a = 2.83$, NM Ni has a low DOS at the Fermi level ($N \approx 21$ states/Ry/atom) and the FM solution is not preferred, whereas DOS of Co and Fe is quite high now ($N = 68$ states/Ry/atom for Co and $N = 48$ states/Ry/atom for Fe) and, therefore, FM ordering is found. At $c/a = 2$ (simple cubic structure), all three metals exhibit very similar and relatively high values of DOS at the Fermi level between $N = 30$ states/Ry/atom and 36 states/Ry/atom. Again, that is why all three metals have FM ordering here. Under further compression the cubic symmetry is lost again and the situation at $c/a = 1.27$ is very similar to the situation at $c/a = 2.83$—low DOS for NM Ni and high DOS for NM Co and Fe. A very high value of DOS for Co at these two points nicely correlates with high magnetic moments and maxima on the curve of the energy difference between FM and NM states. At the bcc structure ($c/a = 1$),

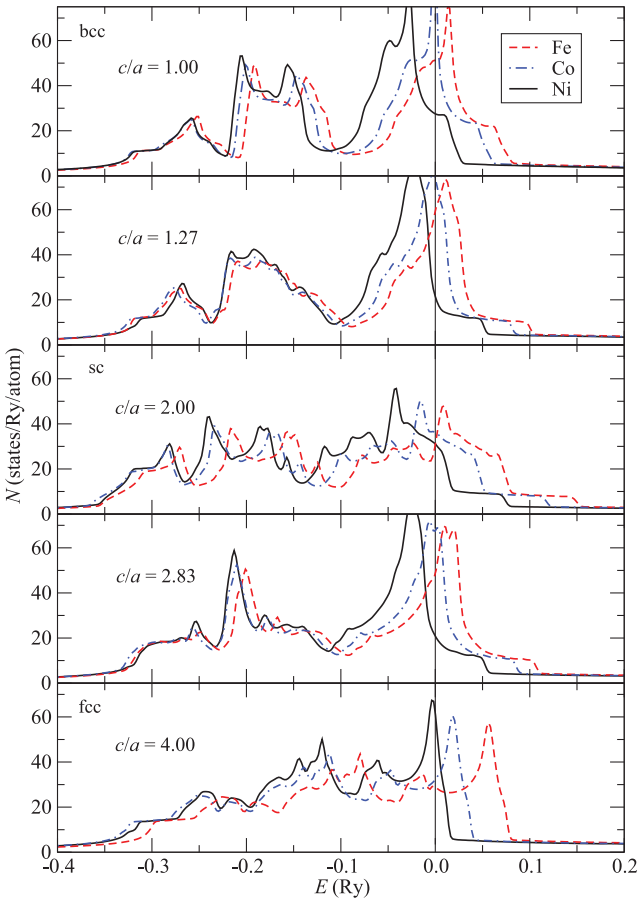

FIG. 6. (Color online) Density of states (DOS) of Fe, Co, and Ni at different points on the trigonal deformation path.

NM Co also exhibits very high DOS, even the highest from all five examples ($N = 90$ states/Ry/atom). DOS at the Fermi level for NM Fe exhibits the second highest value ($N = 51$ states/Ry/atom). Now, the DOS of NM Ni at the Fermi level seems to be relatively small ($N = 28$ states/Ry/atom), but it is sufficient to keep Ni in the FM state. However, already a very small volume compression of bcc Ni leads to a loss of the ferromagnetic ordering, which was also approved by DFT calculations (see, e.g., Refs. 16, 17, and references therein).

V. CONCLUSIONS

In summary, we have calculated the total energies of iron, cobalt, and nickel in various magnetic phases as a function of volume per atom and trigonal deformation and found the phase boundaries between various magnetic modifications in Fe and Ni. In the case of Ni, these phase boundaries occur even at the experimental volume per atom. On the other hand, Co keeps its ferromagnetic order in the whole region of the volume and shape deformation studied. Fe does not exhibit any FM-NM transition, but at low volumes per atom around the fcc structure, phase boundaries between the ferromagnetic high-spin, ferromagnetic low-spin, and antiferromagnetic states have been found.

Areas where Ni loses its FM ordering lie around the values of $c/a = 1.27$ and 2.83 for a large interval of volumes per atom. At the same points, Fe and Co have minima on curves of energy differences between FM and NM states. Both points do not exhibit any higher symmetry structure, but there is a coalescence of the second and third and fifth and sixth coordination spheres ($c/a = 1.27$) or of the third and fourth coordination spheres ($c/a = 2.83$).

Different magnetic behaviors can be explained with the help of an analysis of the density of states at the Fermi level and Stoner theory. It turns out that at the above-mentioned values of c/a, nonmagnetic Ni exhibits a low density of states at the Fermi level, whereas Co and Fe have quite high values. This explains the magnetic orderings found here.

ACKNOWLEDGMENTS

This research was supported by the Grant Agency of the Czech Republic (Project No. 202/09/1786), by the Grant Agency of the Academy of Sciences of the Czech Republic (Project No. IAA100100920), by the Research Project No. AV0Z20410507 of the Academy of Sciences of the Czech Republic, by the Research Project No. MSM0021622410 of the Ministry of Education of the Czech Republic, and by the Project CEITEC–Central European Institute of Technology (CZ.1.05/1.1.00/02.0068) from the European Regional Development Fund. The access to the computing facilities of the METACenter of the Masaryk University, Brno, provided under the Research Project No. MSM6383917201, is acknowledged.

[1] D. A. Young, *Phase Diagrams of the Elements* (University of California Press, Berkeley, 1991), pp. 177–182.
[2] H. Hasegawa and D. G. Pettifor, Phys. Rev. Lett. **50**, 130 (1983).
[3] H. L. Skriver, Phys. Rev. B **31**, 1909 (1985).
[4] P. Söderlind, R. Ahuja, O. Eriksson, J. M. Wills, and B. Johansson, Phys. Rev. B **50**, 5918 (1994).
[5] R. D. Ellerbrock, A. Fuest, A. Schatz, W. Keune, and R. A. Brand, Phys. Rev. Lett. **74**, 3053 (1995).
[6] D. J. Keavney, D. F. Storm, J. W. Freeland, I. L. Grigorov, and J. C. Walker, Phys. Rev. Lett. **74**, 4531 (1995).
[7] S. C. Abrahams, L. Guttman, and J. S. Kasper, Phys. Rev. **127**, 2052 (1962).
[8] A. Onodera, Y. Tsunoda, N. Kunitomi, O. A. Pringle, R. M. Nicklow, and R. M. Moon, Phys. Rev. B **50**, 3532 (1994).
[9] M. Friák, M. Šob, and V. Vitek, Phys. Rev. B **63**, 052405 (2001).
[10] C. S. Tian *et al.*, Phys. Rev. Lett. **94**, 137210 (2005).
[11] G. A. Prinz, Phys. Rev. Lett. **54**, 1051 (1985).
[12] S. M. Valvidares, T. Schroeder, O. Robach, C. Quirós, T.-L. Lee, and S. Ferrer, Phys. Rev. B **70**, 224413 (2004).
[13] H. Giordano, A. Atrei, M. Torrini, U. Bardi, M. Gleeson, and C. Barnes, Phys. Rev. B **54**, 11762 (1996).
[14] E. C. Bain, Trans. AIME **70**, 25 (1924).
[15] M. Šob, L. G. Wang, and V. Vitek, Comput. Mater. Sci. **8**, 100 (1997).

[16]S. Khmelevskyi and P. Mohn, Phys. Rev. B **75**, 012411 (2007).
[17]M. Zelený, D. Legut, and M. Šob, Phys. Rev. B **78**, 224105 (2008).
[18]C. A. F. Vaz, J. A. C. Bland, and G. Lauhoff, Rep. Prog. Phys. **71**, 056501 (2008).
[19]L. Tsetseris, Phys. Rev. B **72**, 012411 (2005).
[20]M. Sambii and G. Granozii, Surf. Sci. **400**, 239 (1998).
[21]M. Zelený and M. Šob, Phys. Rev. B **77**, 155435 (2008).
[22]J. A. Moriarty, Phys. Lett. A **131**, 41 (1988).
[23]M. J. Mehl and D. A. Papaconstantopoulos, Phys. Rev. B **54**, 4519 (1996).
[24]M. Friák *et al.*, Steel Res. Int. **82**, 86 (2011).
[25]D. Legut, M. Friák, and M. Šob, Phys. Rev. Lett. **99**, 016402 (2007).
[26]D. Legut, M. Friák, and M. Šob, Phys. Rev. B **81**, 214118 (2010).
[27]S. Fox and H. J. F. Jansen, Phys. Rev. B **53**, 5119 (1996).
[28]S. Fox and H. J. F. Jansen, Phys. Rev. B **60**, 4397 (1999).
[29]T. Burkert, O. Eriksson, P. James, S. I. Simak, B. Johansson, and L. Nordström, Phys. Rev. B **69**, 104426 (2004).
[30]P. J. Craievich, M. Weinert, J. M. Sanchez, and R. E. Watson, Phys. Rev. Lett. **72**, 3076 (1994).
[31]M. K. Phani, J. L. Lebowitz, and M. H. Kalos, Phys. Rev. B **21**, 4027 (1980).
[32]P. Blaha, K. Schwarz, G. K. H. Madsen, D. Kvasnicka, and J. Luitz, *WIEN2k, An Augmented Plane Wave + Local Orbitals Program for Calculating Crystal Properties* (Karlheinz Schwarz, Technical University of Vienna, Vienna, Austria, 2001).
[33]J. P. Perdew, K. Burke, and M. Ernzerhof, Phys. Rev. Lett. **77**, 3865 (1996).
[34]S. Cottenier, *Density Functional Theory and The Family of (L) APW-Methods: A Step-by-Step Introduction* (Instituut voor Kernen Stralingsfysica, K. U. Leuven, Belgium, 2002).
[35]C. Kittel, *Introduction to Solid State Physics*, 6th ed. (Wiley, New York, 1986).
[36]T. Shimada, Y. Ishii, and T. Kitamura, Phys. Rev. B **81**, 134420 (2010).
[37]*Crystallographic Data on Metal and Alloy Structures*, edited by A. Taylor and B. J. Kagle (Dover, New York, 1963).
[38]M. Mrovec, V. Vitek, D. Nguyen-Manh, D. G. Pettifor, L. G. Wang, and M. Šob, in *Multiscale Modelling of Materials*, edited by V. V. Bulatov, T. Diaz de la Rubia, R. Phillips, E. Kaxiras, and N. Ghoniem, MRS Symposia Proceedings No. 538 (Materials Research Society, Warrendale, PA, 1999), p. 529.
[39]M. Šob, M. Friák, L. Wang, and V. Vitek, Key Eng. Mater. **227**, 261 (2002).
[40]M. Šob, in *Multiscale Materials Modelling: Fundamentals and Applications*, edited by Z. X. Guo (Woodhead, Cambridge, UK, 2007), p. 1.
[41]D. Qian, X. F. Jin, J. Barthel, M. Klaua, and J. Kirschner, Phys. Rev. Lett. **87**, 227204 (2001).
[42]H. L. Meyerheim, R. Popescu, D. Sander, J. Kirschner, O. Robach, and S. Ferrer, Phys. Rev. B **71**, 035409 (2005).
[43]L. M. Sandratskii, Phys. Rev. B **81**, 064417 (2010).
[44]M. Podgórny, J. Magn. Magn. Mater. **78**, 352 (1989).
[45]C. Elsässer, J. Zhu, S. G. Louie, M. Fähnle, and C. T. Chan, J. Phys. Condens. Matter **10**, 5081 (1998).
[46]Z.-Y. Zeng, C.-E. Hu, X.-R. Chen, L.-C. Cai, and F.-Q. Jing, J. Phys. Condens. Matter **20**, 425217 (2008).
[47]E. C. Stoner, Proc. R. Soc. London Ser. A **165**, 372 (1938).